

TIRE MODELING AND CONTACT PROBLEMS

HEAT GENERATION IN AIRCRAFT TIRES

SAMUEL K. CLARK and RICHARD N. DODGE
University of Michigan, Ann Arbor, MI 48109, U.S.A.

Abstract—A method has been developed for calculating the internal temperature distribution in an aircraft tire under free-rolling braked and yawed conditions. The method uses an approximate stress analysis of each point in the tire as it rolls through the contact patch, and from this stress excursion the mechanical work done on each volume element can be converted into a heat release through a knowledge of material hysteresis characteristics. The tire cross-section is considered as an axisymmetric body with internal heat generation, and the heat diffusion equation is solved numerically with appropriate boundary conditions concerning wheel and runway surface. Comparison of data obtained from thermocouple embedded tires shows good agreement.

INTRODUCTION

The development of heavy transport and military aircraft with high performance characteristics has placed increased demand on landing gear and tire components. Specifically, aircraft tires have developed through the years to a point where the ratio of tire weight to aircraft weight has steadily decreased, due in part to improved tire cord materials, rubber compounds and tire structural design. However, as modern aircraft tire operations become more demanding, the strength limits of tire materials are being approached more closely. Thus, a need exists for the development of methods for predicting the strength limit of aircraft tires on some rational basis other than indoor dynamometer testing.

The problem of tire strength differs from that encountered in the strength of normal metallic structures. The reasons for this lie in the complexity of the material characteristics of the constituents in an aircraft tire. In an aircraft tire almost all loads are carried directly by the textile cord reinforcement, commonly nylon as is presently practiced, in the form of a laminated composite shell. Nylon is known to be both non-linear and temperature sensitive. In addition to the strength problem, aircraft tires generate substantial temperatures as they roll, both during takeoff and landing. The temperatures are not high in the usual sense of metallic materials, being on the order of hundreds of degrees Fahrenheit or less, but they are high enough to seriously degrade the strength of the load-carrying textile components of the tires. Excessive temperatures can easily cause a tire to fail even if the stress levels are not overly high.

In addition to the interaction of temperature and stress, even more complex phenomena are at work in the repeated daily use of aircraft tires. These phenomena are basically associated with the long-term strength and adhesion degradation of an aircraft tire due to cyclic variations in stress and temperature. This degradation is an area where not much infor-

mation is available and represents a region where the field usage of tires must depend on experience and judgment rather than science. Because of this strength degradation factor, the useful life of aircraft tires is limited, but these limits are not clearly defined and they vary from one aircraft to another and from one user to another.

Substantial advances are being made in the tire industry in calculating stresses imposed on textile cord structures due to load carrying and inflation pressure. However, the area of tire temperature buildup, which is a major cause of tire failure, has been almost untouched, and there is no analytical technique suitable for predicting aircraft tire internal temperatures on a rational basis. Hence, the tire designer or manufacturer is not able to compare the anticipated temperature buildup in a new design with previous designs or with known temperature-strength characteristics of the materials that he wishes to use. This void is a serious shortcoming in the design process, particularly in the preliminary design of high-performance aircraft tires, where a knowledge of anticipated higher temperatures during normal takeoff and landing cycles would be valuable in assessing the validity of proposed tire aircraft weight and ground speed and taxi-length combinations.

This paper summarizes efforts toward construction of a rational method for evaluating internal temperatures of an aircraft tire and for calculating these rapidly and easily, so that the method may be used as a design tool in both the tire and airframe industries.

ANALYTICAL FORMULATION

The basic material property used in the development of the tire heating computational method is the hysteretic loss characteristic of polymeric materials during cyclic stressing. This characteristic is illustrated in Fig. 1, where a typical stress strain curve for a lossy material is illustrated. As the ma-

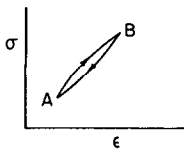


Fig. 1. Typical stress-strain curve of a material illustrating hysteretic loss.

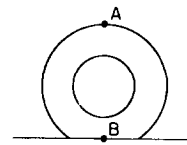


Fig. 2. Extreme points of stress excursion in a tire.

terial is stressed from point A to point B and return, the figure shows that the stress-strain curve of the loading cycle does not coincide with the stress-strain curve of the unloading cycle. The net area under the curve, which remains as the material is returned to its original stress state, represents a loss of mechanical work during the cycle from A to B and return. This lost work is converted into heat and is either diffused through the element and eventually lost from its surfaces or must be accounted for in some way in a heat balance. From an analytical point of view, the work done in a stress cycle as experienced by a material point in passing through the contact patch is expressed most usefully by the use of a simple linear viscoelastic model, such as the Kelvin-Voigt solid, and by using such a model the energy loss per load cycle may be written as

$$\Delta E = U \cdot \pi \Delta V \cdot \tan \delta, \tag{1}$$

where ΔE is the energy loss/cycle, U is the change in strain energy from A to B, $\tan \delta$ is the loss tangent of material and ΔV is the volume element.

This formulation presumes that the initial stress induced by tire inflation has no influence in a linear sense on the energy loss per unit stress cycle. However, the initial stress state may influence the material characteristics, which are not linear in this case.

The method used for calculating the change in strain energy is based on two assumptions. The first is that the tire is made up of a series of material points, each of which undergoes a change in stress state corresponding to the points A and B in Fig. 1, as it moves from point A to B, shown as in Fig. 2.

As a material point moves from A to B in Fig. 2, it is assumed that the general wave form of the stress cycle depicted in Fig. 1 is unimportant, and higher harmonics of the cyclic stress are neglected in favor of a single fundamental cyclic stress change, which will be described in terms of an assumed geometry of the tire at points A and B. In other words, no allowance is made in this simplified analysis for a Fourier decomposition of the stress state as the tire moves from A to B, but rather the fundamental harmonic is considered as defining the change in strain energy between the two points.

The second major assumption made in calculating the strain energy of the tire as it rolls through the contact patch is that at both points A and B of Fig. 2 the cross-section of the tire may be represented geometrically by its neutral axis, around which both membrane and bending strains act.

The inflated shape of the tire is not easy to calculate in any simple fashion since it often exhibits substantial deformations between the inflated and uninflated states. Fortunately, the usual practice is for aircraft tires to carry quite high inflation pressures, and for that reason it is possible to approximate tire cross-section shapes by membrane solutions.

For the deflected tire, a similar but more severe situation exists, since a portion of the cross-section is in contact with the runway. Fortunately, most aircraft tires are molded in the tread and shoulder regions, so a clear line of demarcation is present between portions in contact and portions not in contact. This allows one to assume that the part of the cross-section in contact is flat when at the center of the contact patch, as shown in Fig. 3. The sidewall portion, out of contact, can be defined geometrically by a separate calculation, again using membrane considerations.

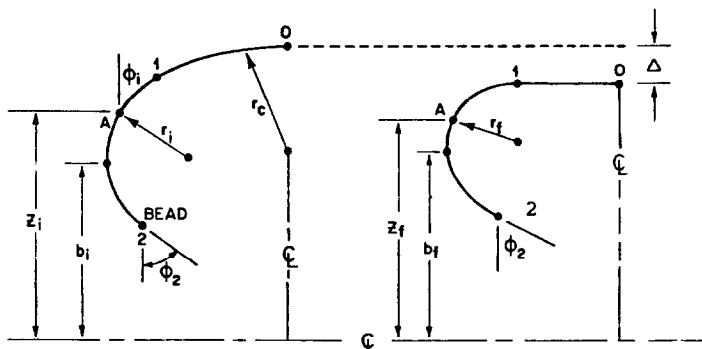


Fig. 3. (a) Assumed geometry at point A of Fig. 2; and (b) assumed geometry at point B of Fig. 2.

Figure 3 illustrates the neutral axis of the structural part of the carcass by the lines labeled 0-1-2. The inflated tire geometry is presumed to be represented by Fig. 3a. The deformed tire, under deflection Δ as shown in Fig. 3b, is presumed to operate under conditions of being perfectly flat when in contact with the runway in section 0-1 and having a reduced radii in the sidewall as given by the symbol r_f . The bead, point 2, is fixed. The regions 0-1 and 1-2 are considered inextensible for computational convenience, which allows the complete geometric description of the various radii of curvature once the tire deflection Δ and the initial tire geometry are given under inflated conditions.

A material point is subject to both bending and membrane strain during deformation of the tire from point A to point B, as shown in Fig. 2. The bending strains depend on the radius of curvature of the tire carcass midline, as illustrated in Fig. 3, as well as on the distance from this carcass midline. The bending strain can be calculated in the usual Kirchoff fashion based on knowledge of change in radius of curvature of the carcass midline between the two points in question in Fig. 2.

Membrane strains also exist in the tire cross-section due to the high-inflation pressure commonly used in aircraft tires. Some of these membrane strains are not directly obtained from the geometric changes that have been postulated, since they depend heavily on contact patch boundary conditions. Other membrane strains must be obtained from a knowledge of the membrane stresses in the tire. These membrane stresses in turn depend on the curvature characteristics of the tire as well as on geometric variables that may be calculated from the tire cross-section geometries given in Fig. 3. In particular, the sidewall area must be carefully defined since the point of vertical tangency of the tire is an important factor in computation of membrane stresses. This point of vertical tangency, measured as the distance b in Fig. 3, shifts during the deformation process, and the position of the various material points relative to this point of vertical tangency must be tracked in the subsequent computations.

Bead tensions also change during the deformation process and must be incorporated into a cyclic stress mechanism involving a loss characteristic of the bead itself. These bead tensions depend on the angle of tangency of the side wall at the bead, denoted as point 2 in Fig. 3.

For purposes of computing changes in strain energy states during the cyclic loading process, the tire is divided into five regions, denoted as I-V in Fig. 4. Referring to Fig. 4, regions I and III represent carcass material, which may be considered an angle ply composite with the usual composite elasticity characteristics in the meridional (ϕ) and circumferential (θ) directions. Regions II and IV are an isotropic rubber covering on the carcass—region II being that portion in contact with the roadway, i.e.

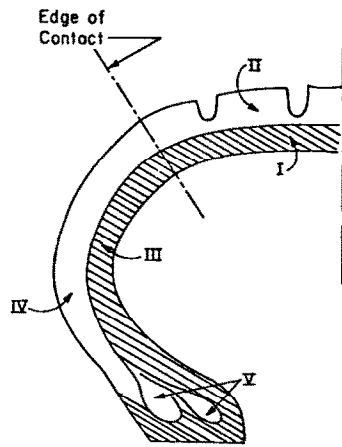


Fig. 4. Tire cross-section showing regions of different characteristics and loading patterns.

the tread, while region IV is the sidewall covering. Region V is the bead, which is treated separately. Individual regions are considered in light of the known geometry changes that the tire must undergo to conform to the imposed deformation while in contact with a flat surface. Membrane and bending stresses may be determined in both regions I and III, i.e. the carcass, and these may be used with the appropriate composite elastic constants to determine the membrane and bending strains. This allows strain energy density to be calculated in those regions.

Region II, the tread area, is taken to have the same membrane strain as the underlying carcass material, which is of course much stiffer, but is in addition acted upon by the compressive stresses associated with the pressure distribution in the tread. This allows the energy density in the tread region to be calculated.

Finally, region IV, representing the isotropic sidewall material, is assumed to follow the strain pattern of its surface of contact with the underlying carcass material. Due to the angle ply nature of aircraft tire construction, the meridional membrane stress strongly influences the circumferential membrane stress. In view of the fact that these meridional membrane stresses are, in turn, defined by radii of curvature that change rapidly during passage of the tire sidewall through the contact patch, it is also true that the circumferential membrane forces change rapidly in that region. This in turn causes fluctuating membrane shear stresses to exist in the sidewall area, and these must be included in calculating the total membrane stress state of the tire sidewall.

A detailed exposition of the analytical formulations for strain energy density under these various conditions is given in Ref. [1].

HEAT GENERATION AND HEAT FLOW

Based on the well-known complex representation of stress response under oscillating sinusoidal strain

at a frequency corresponding to the fundamental frequency of stress cycling in the tire, as given by eqn (2), the energy loss per cycle is represented by

$$W = \pi U \tan \delta, \quad (2)$$

where U is the change in elastic strain energy during the cyclic stressing process and W is the work done (energy lost) per cycle. Values of $\tan \delta$ are not readily available for commercial cord rubber composites, but preliminary experimental work done at the University of Michigan on selected samples gives approximate average values that can be used for purposes of estimating heat generation rates.

Converting the expression for work done per unit volume of material per cycle of stressing into a heat generation rate requires insertion of the tire-rolling velocity, rolling radius r_0 and a number of thermal constants as well as conversion to proper units. Making these changes, one obtains an equation for the heat generation rate in cal/cm³/sec in the form of

$$\dot{q} = 0.01 \frac{U v_0 \tan \delta}{r_0 - \Delta/3}, \quad (3)$$

where r_0 is the outside radius of tire (in.), Δ is the tire deflection (in.), v_0 is the aircraft velocity (ft/sec) and U is the elastic energy (in.-lb/in.³) stored due to the change in stress state.

TEMPERATURE DISTRIBUTION MODEL

The temperature distribution model is illustrated in Fig. 5. The heat conduction cells are chosen to coincide with natural boundary lines between the tread and carcass and natural geometric divisions of the tire shape. This allows the properties of each cell to be uniform, which is a considerable convenience in subsequent calculations. The stress state in each cell is calculated on the basis of the centroidal characteristics of the cell and is averaged over the cell volume. Quadrilateral elements have been consistently utilized in constructing the numerical analog to this solution. Each element loses or gains heat from four faces, and this exchange may be through conduction when the element is bounded by similar elements, or by convection

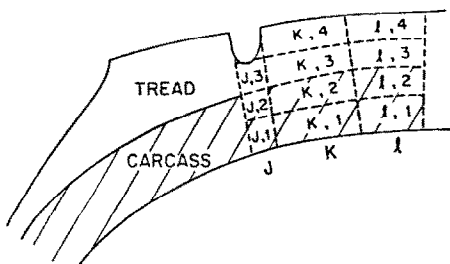


Fig. 5. Distribution of computational elements in the tread region.

from surface faces, or by conduction to either the flange of the wheel or to the runway surface for those special elements that come in contact with them.

The heat diffusion equation under conditions of internal heat generation is shown in eqn (4).

$$K \nabla^2 \theta = \rho \frac{\partial \theta}{\partial t} - \dot{q}. \quad (4)$$

This expression may be written for finite difference purposes in the form

$$\begin{aligned} \frac{\Delta \theta}{\Delta t} = & \dot{q} + \bar{\alpha}_{K-1,K} (\theta_{K-1,l} - \theta_{K,l}) \\ & + \bar{\alpha}_{K,K+1} (\theta_{K+1,l} - \theta_{K,l}) \\ & + \bar{\alpha}_{K,l-1} (\theta_{K,l-1} - \theta_{K,l}) \\ & + \bar{\alpha}_{K,l,l+1} (\theta_{K,l+1} - \theta_{K,l}), \end{aligned} \quad (5)$$

whose elements are illustrated in Fig. 5 and where $\bar{\alpha}_{m,n} = KA/d$; K is the thermal conductivity, A is the area of contact between subscripted elements and d is the distance between centroids of subscripted elements.

The basic method of computation is to use small time increments and to calculate the temperature rise in each cell utilizing the temperatures of adjoining elements from the previous time increment computation. There are several factors that make this type of computation possible. First, it is well known in heat transfer calculations that if the quantity given by the expression $M = \Delta x^2/a\Delta t$, where a is the \dot{q}/α , Δx is the element size and Δt is the time increment is large, then stability of such a time-based forward computation is assured and convergence to correct results will be obtained. For this reason, cell elements have been kept moderately large and time increments small, since this reduces requirements for computer memory and also ensures stability of the computation. Second, the dominant term is the rate of heat generation \dot{q} , and for purposes for aircraft taxi and takeoff the heat buildup occurs over a relatively short period of time, so that the heat generation term almost completely controls the temperature rise in the tire. Heat diffusion, at least for the takeoff case, is a minimal effect. Thus, heat conduction using adjoining cell temperatures from the previous time interval incurs only very small errors in the final temperature distribution in the tire.

The heat transfer coefficients from tire to air are not particularly well known in this case, but again it is fortunate that taxi takeoff cycles are relatively short, so that again the rate of internal heat generation is the dominant term. However, in studying taxi and combined taxi takeoff operations, more emphasis is placed on the accuracy of the heat transfer and heat conduction coefficients associated with this problem. In that case those coefficients become more important.

The method of temperature computation using eqn (5) now consists of starting from whatever initial temperature state one wishes in each of the cells, allowing a short time interval to take place and computing the heat generated in each cell using the concepts outlined above. In carrying out such computations, knowledge of the material loss characteristic $\tan \delta$ is needed.

At the end of the first time interval the temperature field in the entire tire is calculated and is used as a basis for the heat transfer characteristics during the second time interval, which follows immediately. The computation is sequential, thus requiring minimum memory storage in a computer, and may conveniently be carried out on relatively unsophisticated equipment such as minicomputers.

The contained air temperature in the tire is often measured and used as an indication of overall tire heating. Its calculation requires a separate analysis. From this analysis the contained air temperature can be shown to lag behind the inner surface temperature of the tire. In the initial stages of tire heating, its value is given by

$$\Delta y = \beta \Delta t (\theta - y), \quad (6)$$

where y is the contained air temperature, θ is the weighted average of tire inner surface temperatures, Δt is the time increment and β is a constant involving properties of the air and heat transfer coefficients.

BRAKED AND YAWED ROLLING

The approximate stress analyses and heat generation discussed above pertain primarily to the free-rolling tire in straight line motion. However, other conditions of tire operation require additional analyses. The most important of these are braking and yawed rolling.

Considering first the case of braked rolling conditions, where the tire itself undergoes different stress conditions than in the free-rolling case. It is most direct to consider these as additions to the free-rolling case. These take several forms. First, it may be shown that in any braked tire a certain level of surface slip occurs between the tread surface of the tire and the runway. The exact amount of slip is difficult to quantify since there is some elastic deformation of the tire carcass, which gives the appearance of slip and yet is not actually physical motion of the tread surface relative to the runway. However, a careful analysis of this slip phenomena as given in Refs. [2] and [5] shows that the work done per tire revolution associated with slip phenomena is

$$\begin{aligned} W &= F_x (\text{slip distance per revolution}) \\ &= \frac{F_x^2 \pi D}{F_z C_8}, \end{aligned} \quad (7)$$

where F_x is the brake force, D the tire diameter, F_z the normal force and C_8 a constant related to tire fore-aft stiffness. This may be converted to the rate of heat release in cal/sec by using appropriate numerical constants to give

$$\dot{Q} = \frac{0.32 F_x^2 v_0}{C_8 F_z}, \quad (8)$$

where \dot{Q} is the total heat release rate due to tire slip (cal/sec) and v_0 is the aircraft velocity (ft/sec). It is assumed that this is uniformly distributed throughout the tread region of the tire.

Note that the rate of heat generation due to slip is proportional to the square of the braking force. This prediction was later borne out by appropriate experimental studies.

In addition to the surface scrubbing effects described above, braking of the tire also induces additional stresses in the tire itself. These stresses take two forms. The first is additional shear stress in the carcass underneath the tire tread itself. These shear stresses are primarily concentrated in the contact area of the tire and result in increased tensions at the forward edge of the contact patch and decreased tensions at the rear edge. These additional carcass stresses are distributed through the carcass sidewall tire and eventually into the tire beads and wheel. Due to the angle ply laminate nature of the sidewall construction, the shear stresses involved diffuse rapidly and become quite small by the time they reach the upper sidewall area.

For purposes of yawed rolling, further modifications must be made to the free-rolling tire analysis program previously described, since four additional physical phenomena must be considered. The first of these is lateral displacement of contact elements in the tire tread away from their normal symmetric position. This causes substantial changes in the radii of curvature of the tire sidewalls, and this new geometry must be used in conjunction with the tire vertical deflection in order to define the radii of curvature of the tire at its most extreme deflected position. The radii of curvature on each side of the tire are no longer the same, so it is to be expected that one side of the tire will generate more heat than the other side.

A second major effect in the yawed tire is lateral sliding of the tire surface on the runway at the rear of the contact patch. This phenomenon is well known since it has been studied extensively in passenger tire cornering phenomena. It results in a surface heat release similar to that associated with the braking problem.

Finally, two sets of additional stresses are introduced into the tire by virtue of the lateral forces associated with yawed rolling. The first of these is the lateral cyclic shear stress components in the tread elements arising from the lateral frictional forces associated with cornering in the contact patch. These may be calculated by conventional

methods and used in the resulting computer program. These lateral shear forces pass through not only the tread elements of the tire but also into the carcass region of the tire immediately underneath the tread elements. This generates additional heat in the carcass elements. Finally, these forces are carried through the sidewalls, but due to the diffusion characteristics of angle ply composite laminates discussed earlier, such lateral forces decay rapidly as they approach the bead region.

All of these effects have been included in two separate subroutines of the main program written to describe general heat generation in aircraft tire operation. One subroutine introduces the concept of the braking force in straight line motion and the second introduces yaw characteristics as desired.

THERMOELASTIC MATERIAL PROPERTIES

It is recognized that the computations described in this paper require adequate thermoelastic properties for implementation. Unfortunately, data concerning cord rubber composites are sparse in the literature, and in many cases estimates must be made from data on pure rubber compounds in order to obtain the necessary numerical information.

Among other physical properties needed are the following: composite thermal conductivity; composite elastic constants, including both real and imaginary modulus or real modulus and $\tan \delta$; heat transfer coefficients from the tire surface; thermal

contact resistance between the tire and the runway; thermal contact resistance between the tire and the aluminum wheel; and knowledge of airflow velocities both inside and outside the tire.

Of these various constants, the single most important one in terms of the heat generation problem being studied here is that of the loss characteristics of the cord rubber composites used for the carcass of the tire. Little information is available on loss characteristics of cord rubber composites. However, it is known that such characteristics are quite temperature sensitive, and their behavior is one of the primary reasons for the essentially stable temperature characteristics of an operating tire under steady-state running. Unfortunately, they are also sensitive to frequency as well as to other characteristics such as strain amplitude and prestrain level. A search of the pertinent literature revealed very little useful information in this regard, but because of the importance of its temperature and frequency dependence, an empirical expression has been generated and is currently being used to link the thermal and elastic characteristics of the composite carcass structure. This formulation is given as

$$\tan \delta = c_0 + c_1 \frac{1 + c_2 \log [v_0/2\pi(r_0 - \Delta/3)]}{\theta} \quad (9)$$

where c_0 , c_1 , c_2 are constants, v_0 is the aircraft velocity, θ is the temperature of point at which $\tan \delta$

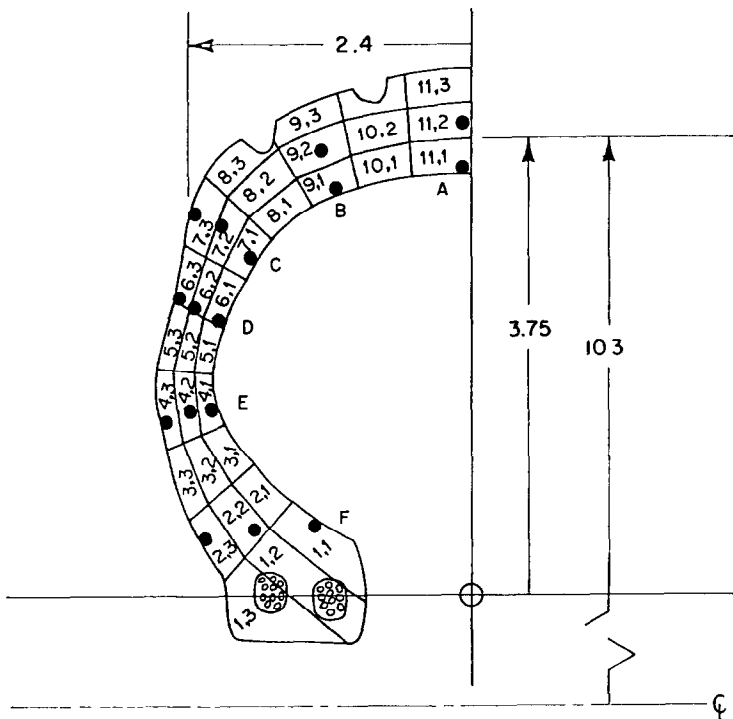


Fig. 6. Element sectioning for thermal analysis. Large solid circular symbols represent approximate thermocouple locations in the 22×5.5 12 PR test tires.

is to be found, r_0 is the tire radius and Δ is the tire deflection. Other elastic and thermal characteristics are approximated by their room temperature values, such as given in Ref. [4].

EXPERIMENTAL PROGRAM

A comprehensive experimental program was carried out at the University of Michigan jointly with the Impact Dynamics Branch, Langley Research

Center, National Aeronautics and Space Administration, Hampton, VA, in order to obtain data on 22×5.5 8 PR and 12 PR tires for use in comparison with calculations on temperature rise using the methods described here. Thermocouples were installed in tires at locations given by Fig. 6. The tire was operated under a variety of conditions in order to compare measured temperature rises with those calculated from the program. In addition, the University of Michigan instrumented 40×14 22 PR

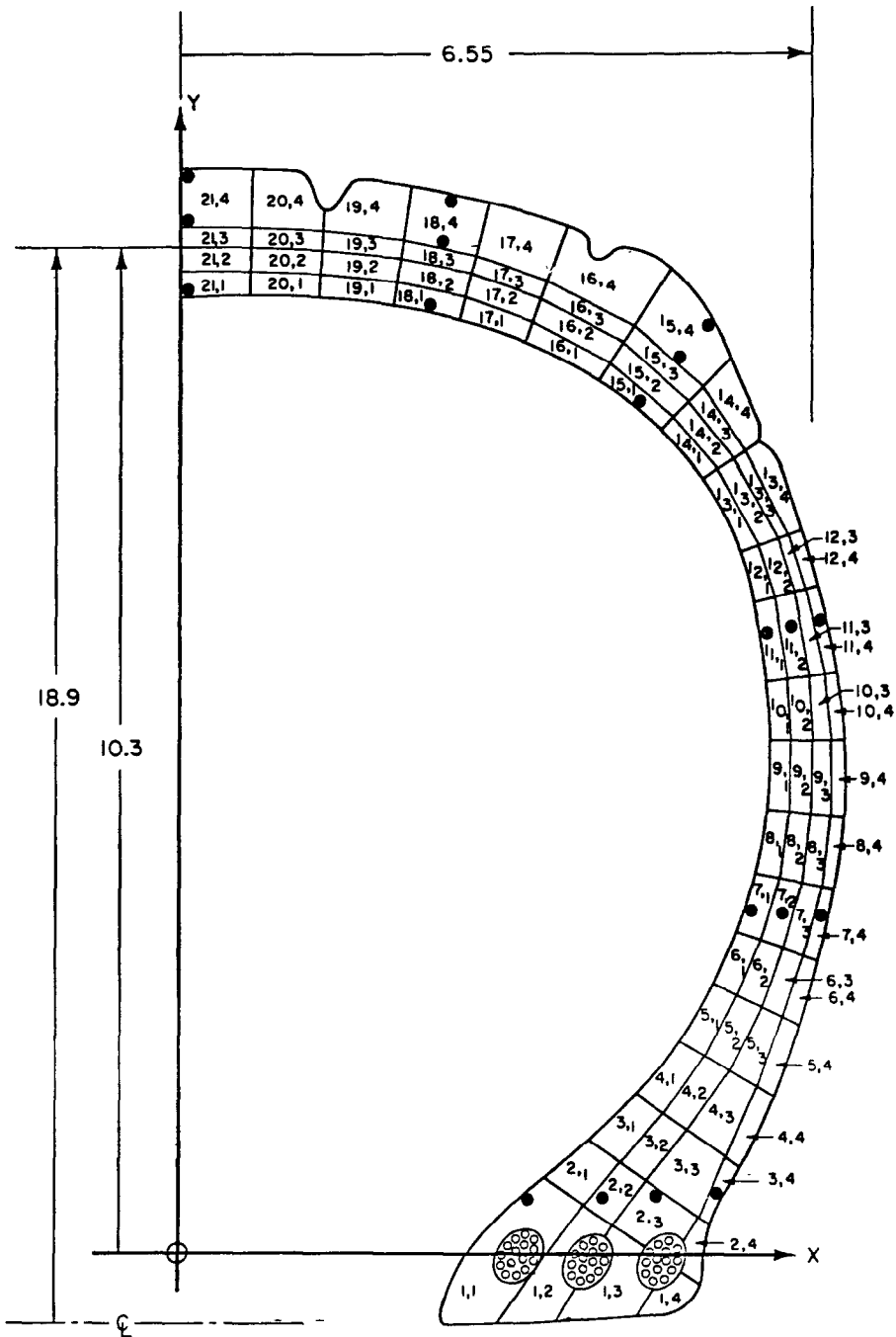


Fig. 7. Element sectioning for thermal analysis. Solid circular symbols represent approximate thermocouple locations in the 40×14 28 PR test tires.

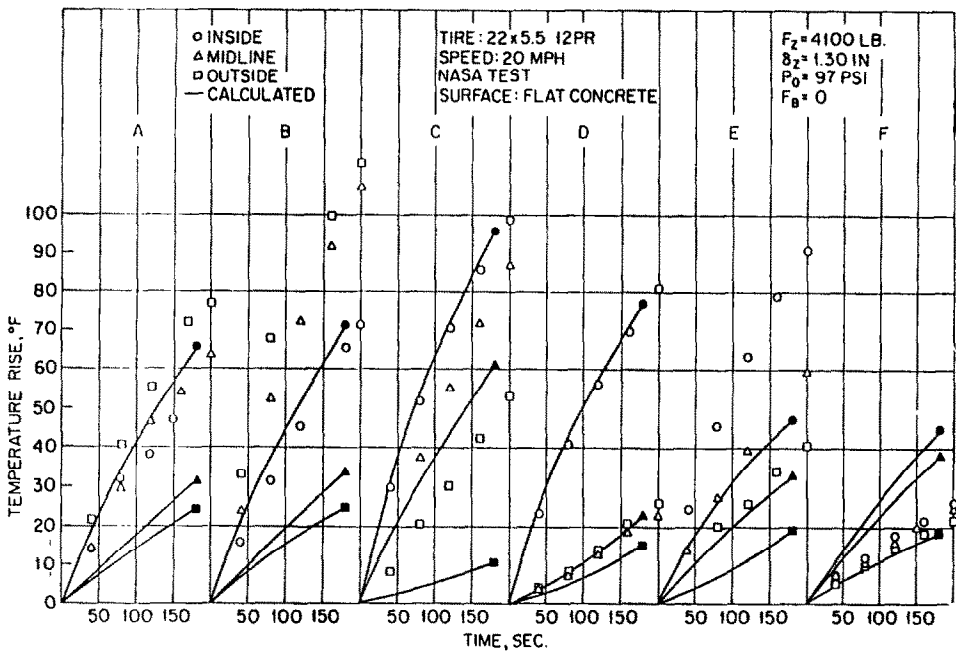


Fig. 8. Measured and calculated tire temperature profiles for a rolling tire.

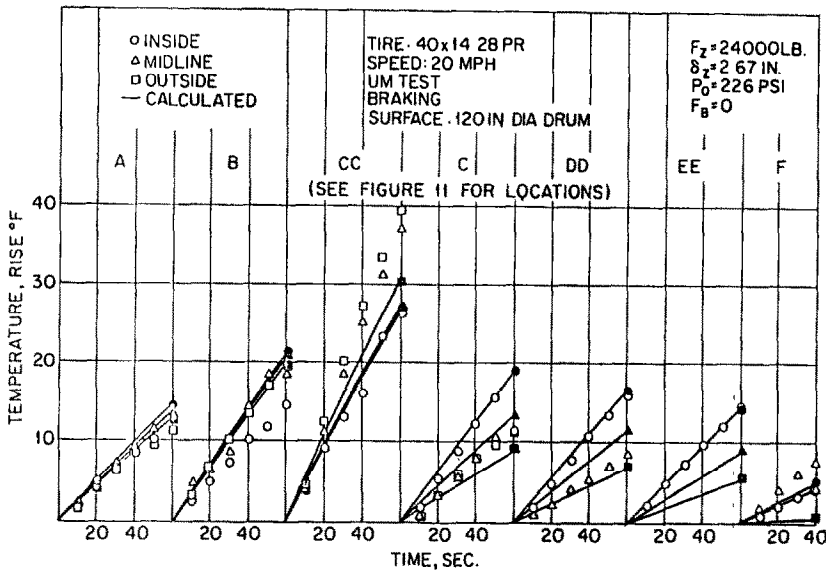


Fig. 9. Measured and calculated tire temperature profiles for a free-rolling tire.

and 28 PR tires, which were also run under a variety of conditions at the test facilities of the Air Force Flight Dynamics Laboratory, Wright-Patterson Air Force Base, Ohio. Thermocouple locations are shown in Fig. 7 for use in comparison with subsequent calculations. Typical comparisons of calculations and experiment results are given in Fig. 8 for the smaller tire and in Fig. 9 for the larger tire, both for free-rolling conditions. These illustrate the fact that the calculated values seem to approximately represent the temperature observed.

Similar experimental studies were done on the influence of tire braking on temperature rise. Again, the same two sizes of tires were used, and again the NASA Langley test equipment was used for measurement of temperature rise characteristics for the smaller tire. This is illustrated in Fig. 10, where it is shown that rather substantial temperature rise now occurs in the tread region of the tire when it is heavily braked. Data is from Ref. [3].

The larger 40 x 14 tire was again instrumented at the University of Michigan and operated under

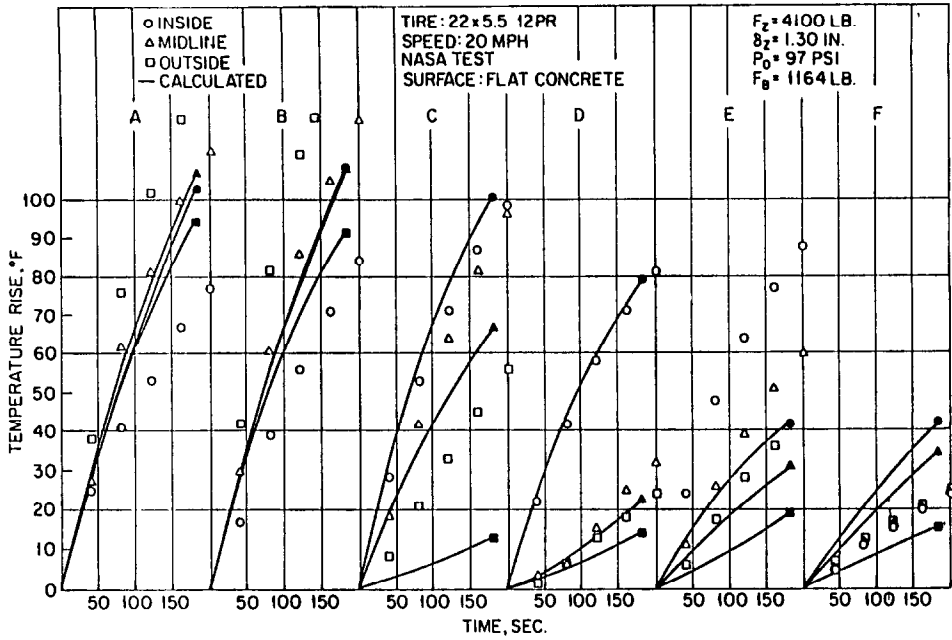


Fig. 10. Measured and calculated tire temperature profiles for a braked tire.

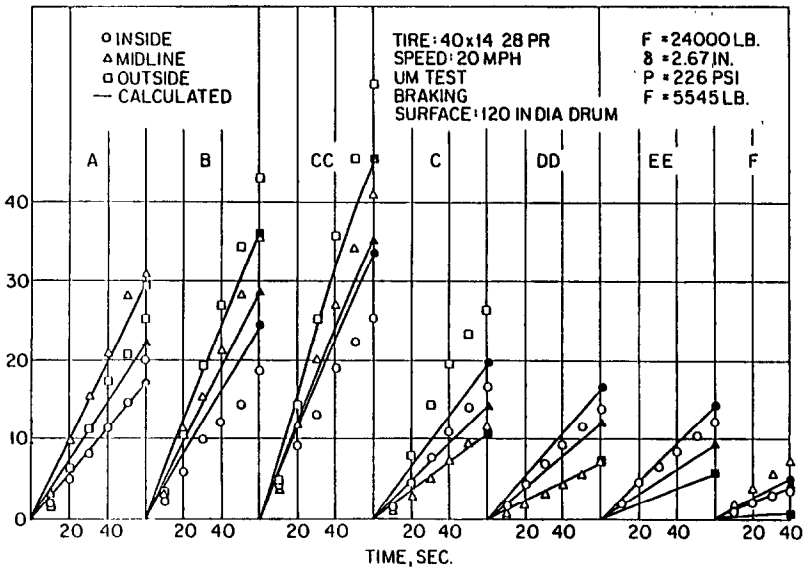


Fig. 11. Measured and calculated tire temperature profiles for a braked tire.

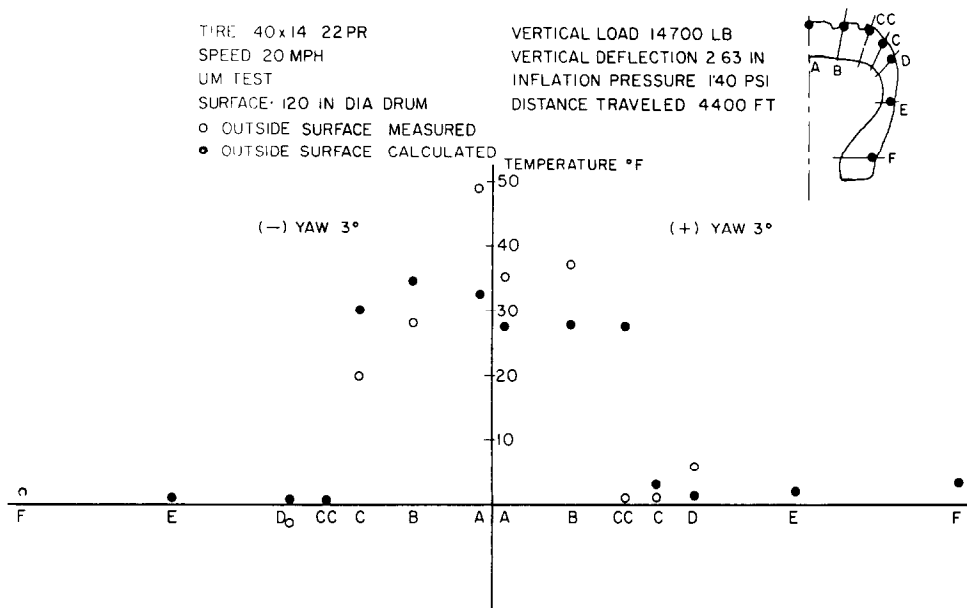


Fig. 12. Influence of cornering direction on temperature rise above free-rolling conditions; 40 × 14 tire.

braked rolling conditions. This is shown in Fig. 11, where it is seen that trends are predicted fairly well.

Yawed rolling experiments have also been carried out quite recently, again to corroborate the calculated values. Here emphasis was on verifying some of the more detailed predictions of the calculations, such as differences between the temperature rise on opposite sidewalls of the yawed tire. These results are illustrated in Fig. 12 for the larger tire and show a certain amount of temperature asymmetry in both calculations and experiments.

CONCLUSIONS

A method has been developed for approximating the internal temperature distribution in an aircraft tire due to unyawed free rolling under load, braked rolling under load and yawed rolling without braking conditions. The method is based on an approximate stress analysis of a material point in the tire as it rolls through the contact patch. From this analysis the mechanical work done on the material point is converted into the heat generated due to the loss characteristics of the materials in tire construction. The resulting tire temperature distribution is considered to be axisymmetric, and a numerical solution to this problem has been coded as a relatively simple time-forward integration process for the temperature state in the tire.

An extended experimental program was carried out jointly by the University of Michigan and the Impact Dynamics Branch, Langley Research Center, NASA, in order to measure temperature characteristics of both the free-rolling braked and yawed tires. Data were obtained from thermocouples buried in the tire carcass prior to retreading the tires. Experimental data from these measurements were compared with data calculated over a wide range of tire loads, inflation pressures, speeds and deflections. Generally speaking, the analytical model gives good agreement with measured values when the tire is operating in the range of its normal rated load, pressure and deflection.

REFERENCES

1. S. K. Clark and R. N. Dodge, Heat generation in aircraft tires under free rolling conditions. NASA CR-3629 (1983).
2. J. A. Tanner, Fore-and-aft elastic response characteristics of 34 × 9.9, type VII, 14 ply-rating aircraft tires of bias-ply, bias-belted, and radial-belted design. NASA TN D-7449 (1974).
3. J. L. McCarty, Wear and related characteristics of an aircraft tire during braking. NASA TN D-6963 (1972).
4. J. W. Walter, Cord rubber tire composites. *Rubber Chem. Tech.* 51(3), 524 (1978).
5. S. K. Clark and R. N. Dodge, Heat generation in aircraft tires under braked rolling conditions. NASA CR-3768 (1984).